AIAA JOURNAL
Vol. 47, No. 5, May 2009

Vortex Roll-Up Criterion for Synthetic Jets

Jue Zhou,* Hui Tang,* and Shan Zhong†
University of Manchester, Manchester, England M60 1QD, United Kingdom

DOI: 10.2514/1.40602

In this paper, both theoretical analysis and numerical simulations are undertaken to study the parameters that affect the strength of vortex roll-up of synthetic jets. A dimensional analysis reveals that the dimensionless vorticity of vortex roll-up produced by an orifice flow depends on the dimensionless stroke length, Stokes number, and the ratio between the orifice diameter and the thickness of the Stokes layer. Based on the results from a fully developed oscillating laminar pipe flow, the Stokes number is found to play an important role in determining the thickness of the Stokes layer inside the orifice and hence the shape of the velocity profile. Results from the numerical simulations confirm that the Stokes number also determines the strength of vortex roll-up of a synthetic jet issued from an orifice of a finite depth, for the same reason. Finally, a parameter map, which marks the three different regimes of synthetic jets (classified as no jet, jet formation without vortex roll-up, and jet formation with vortex roll-up) is produced based on the numerical simulation results. It is shown that for the synthetic jet actuator used in the present study, a minimum Stokes number of about 8.5 is required to ensure the occurrence of an appreciable vortex roll-up at a dimensionless stroke length greater than 4. In addition, a very low Stokes number can also suppress the formation of synthetic jets. This study provides a further understanding of the behavior of synthetic jets in quiescent conditions, which will be useful for designing more effective synthetic jet actuators in which vortex roll-up is desired.

Nomenclature

D_c	=	cavity diameter, m
D_o	=	orifice diameter, m
f	=	diaphragm oscillation frequency, Hz
H	=	cavity depth, m
h	=	orifice depth, m
L	=	dimensionless stroke length, L_o/D_o
L_o	=	stroke length, $\bar{U}_o T$, m
Re_L	=	Reynolds number based on the stroke length, $\bar{U}_o L_o/\nu$
r	=	radial coordinate measured from the center of the diaphragm or orifice, m
S	=	Stokes number, $\sqrt{2\pi f D_o^2/\nu}$
T	=	period of diaphragm oscillation cycle, s
t	=	time, s
$\bar{U}_o$	=	time-averaged jet blowing velocity over the entire cycle, m/s
u	=	instantaneous jet exit velocity, m/s
x	=	axial coordinate measured from the orifice exit, m
Δ	=	peak-to-peak displacement at the center of diaphragm, m
ν	=	molecular kinematic viscosity, m^2/s

I. Introduction

A VORTEX ring is usually formed by ejecting fluid impulsively from an orifice [1]. A vortex sheet separates at the edge of the orifice and rolls up to form a vortex ring, which moves downstream with a self-induced translational velocity. Vortex rings produced by means of an impulsively started piston have been well studied, with the earliest publications dating back to the 1850s. Research has been undertaken both numerically and experimentally to investigate how the characteristic parameters of fully formed vortex rings, such as the ring diameter, the circulation, and the translational velocity change with the nozzle geometry, the piston stroke, and the velocity history of the piston movement [2–5].

In recent years, more research attention has been given to synthetic jets due to their potential for flow separation control in aerospace applications [6–9]. A typical synthetic jet actuator consists of a small cavity with an oscillating diaphragm at its bottom side and an orifice plate at the opposite side, as shown in Fig. 1. As a result of the alternating of suction and blowing produced by the movement of the diaphragm, a succession of vortex rings is produced and propagates away from the orifice.

The vortex rings produced by a synthetic jet actuator differ from those produced by a piston arrangement in that the behavior of the former is strongly affected by the presence of a suction flow in the neighborhood of the orifice. As a result, a synthetic jet will only form when the vortex ring is able to overcome the suction velocity during the ingestion stroke. Holman et al. [10] defined synthetic jet formation as the appearance of a time-averaged outward velocity along the jet axis that corresponds to the generation and subsequent convection of vortex rings. Based on their numerical and experimental studies, a formation criterion for both two-dimensional and axisymmetric synthetic jets was proposed. It was stated that for the synthetic jet to form, the reciprocal of the Strouhal number $1/Sr = \bar{U}_o/\pi f D_o$ should be greater than a threshold value K, where the constant K depends on geometric factors such as orifice/slot shape, radius of curvature, and aspect ratio of the slot. For axisymmetric synthetic jets, K is found to be equal to 0.16. Taking into account the relationship between the Strouhal number and the dimensionless stroke length, the preceding criterion can be translated into a dimensionless stroke length of about 0.5 for axisymmetric synthetic jets. A different value ($\approx$0.25) was given by Milanovic and Zaman [11]. The difference in the threshold was attributed to factors such as the differences in the lip shape of the orifice and the diaphragm velocity program.

Vortex rings are known for their ability to entrain ambient fluid into their cores, which enhances mixing. When a synthetic jet is issued into a boundary layer, the injection of coherent vortices via the initial vortex roll-up results in formation of a hierarchy of vortical structures that are capable of delaying flow separation [12,13]. It is understandable that the strength of vortex rings in terms of the level of circulation will determine the impact of synthetic jets on the external flow. A question remains, however, if a synthetic jet that satisfies the aforementioned formation criterion will definitely have a vortex roll-up. Guo and Zhong [14] studied the behavior of synthetic jets issued from an orifice of 5×10^{-4} m diameter and observed no vortex roll-up at a dimensionless stroke length of 4 and a Stokes number of 7. This prompted them to investigate the conditions for

Received 26 August 2008; revision received 12 February 2009; accepted for publication 6 February 2009.

*Postgraduate Researcher, School of Mechanical, Aerospace and Civil Engineering, George Begg Building, Sackville Street.
†Senior Lecturer. Senior Member AIAA.

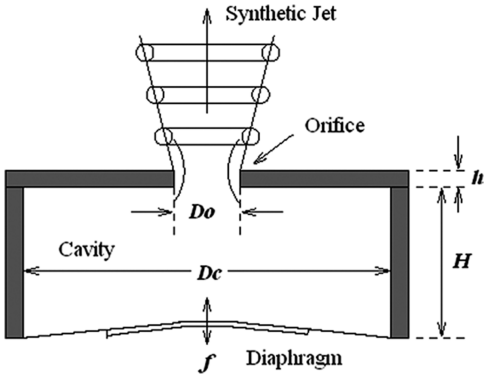

Fig. 1 Schematic of the synthetic jet actuator.

vortex roll-up by conducting particle image velocimetry (PIV) measurements on a synthetic jet issued from an orifice of 5×10^{-3} m diameter. They found that the Stokes number is an important parameter that determines the strength of roll-up, because it affects the shape of the velocity profile at the orifice exit. Based on a qualitative observation of their experimental results, it appears that a minimum Stokes number of about 10 is required for an appreciable roll-up to occur at a dimensionless stroke length of around 4. Nevertheless, a more in-depth examination of this criterion is still needed to provide a theoretical backup and evidence of validation.

To ensure the flow control effectiveness of synthetic jets in practical settings, a better knowledge of the parameters that affect the formation of these vortex rings is required. To the best knowledge of the authors of this paper, however, although there has been a volume of research work on the roll-up process of vortex rings produced by a single pulsation of a piston [1–4], the conditions for roll-up of vortex rings produced by synthetic jets have not been reported in the literature. In this paper, both dimensional analysis and numerical simulations are therefore undertaken to investigate the vortex roll-up criterion for synthetic jets issued into quiescent air. The dimensional analysis identifies the parameters that determine the extent of vortex roll-up. Numerical simulations were then undertaken to illustrate how these parameters affect the formation and strength of vortex roll-up for a 5-mm-diam synthetic jet. Finally, a parameter map, which marks the three different regimes of synthetic jets classified as no jet, jet without roll-up, and jet with vortex roll-up, is produced based on the numerical simulation results. The finding from this study is expected to be useful to the design of synthetic jet actuators for which formation of vortex rings is desired.

II. Computational Methods

In this study, a synthetic jet actuator identical to that used by Guo and Zhong [14] in their experiment is chosen as the model for the simulations (see Fig. 1). The actuator has a cylindrical cavity with a diameter $D_c = 4.5 \times 10^{-2}$ m and height $H = 1 \times 10^{-2}$ m. Its orifice has a diameter $D_o = 5 \times 10^{-3}$ m and depth $h = 5 \times 10^{-3}$ m, giving an orifice depth-to-diameter ratio h/D_o of 1. This particular orifice depth-to-diameter ratio is chosen because it is near the optimal value that was found to produce the maximum vortex circulation for an actuator of a similar design [8]. In the experiment, the thin rubber diaphragm, which is sandwiched between two metal disks, is clamped circumferentially to the end of the cylindrical cavity, and the center of the diaphragm is attached to a permanent magnetic shaker via a steel rod. The diaphragm is made to oscillate in a sinusoidal manner at predetermined diaphragm oscillation displacements and frequencies. At small displacements, this diaphragm mimics the motion of an oscillatory piston.

Unsteady incompressible laminar flow simulations are performed using a commercial solver, FLUENT 6.2. To simplify the computation, the flow is treated as axisymmetric. The flow in both the orifice and actuator cavity are included in the simulation to ensure the accuracy of the results. The computational geometry and the boundary conditions used in the simulation are shown in Fig. 2. To ensure adequate spatial resolution of the flow structures, the grids are densified in the actuator orifice, the region around the jet central plane, and near the walls. The entire computational domain contains 23,660 mesh cells. The time step used in the simulations is $T/80$. A sensitivity study undertaken previously showed that the choices of mesh size and time step used in the present study are adequate [15].

In the present study, the instantaneous displacement relative to its neutral position of the oscillating diaphragm is given by

$$\delta(t) = \frac{\Delta}{2}\sin(2\pi f t) \tag{1}$$

where δ is the deformation of the diaphragm relative to its neutral position, and Δ is the peak-to-peak displacement of the diaphragm. To simplify the computation, a velocity boundary condition is applied at the neutral position of the diaphragm. The moving velocity of the diaphragm can be obtained by differentiating Eq. (1) with respect to time:

$$v(t) = \pi \Delta f \cos(2\pi f t) \tag{2}$$

The velocity boundary condition is specified using user-defined functions supported by FLUENT.

The numerical method has been validated using data measured with PIV and a hot wire by Tang and Zhong [15]. Two figures extracted from their paper illustrating the good agreement between the predicted and measured instantaneous jet centerline velocity and jet exit velocity profile are shown in Fig. 3. It is evident that the computational software with the setting used in this study is capable of reproducing the key characteristics of synthetic jets observed in the experiments.

III. Dimensionless Parameters of Synthetic Jets

The behavior of synthetic jets issued into a quiescent flow is usually characterized by three nondimensional parameters: the dimensionless stroke length L, the Reynolds number Re_L based on stroke length, and the Stokes number S [8]. The stroke length of a synthetic jet represents the length of a fluid column that is pushed out during an actuation cycle: that is [4],

$$L_o = \bar{U}_o T \tag{3}$$

where $\bar{U}_o$ is the time-averaged blowing jet velocity over an entire cycle and T is the oscillating period. It defines an important dimensionless parameter for synthetic jets called the dimensionless stroke length:

$$L = \frac{L_o}{D_o} = \frac{\pi}{Sr} \tag{4}$$

The Reynolds number defined based on the time-averaged jet velocity $\bar{U}_o$, and the stroke length L_o is given by

$$Re_L = \frac{\bar{U}_o L_o}{\nu} \tag{5}$$

where ν is the kinematic viscosity coefficient. Re_L is often regarded as important because it is proportional to the total circulation ejected

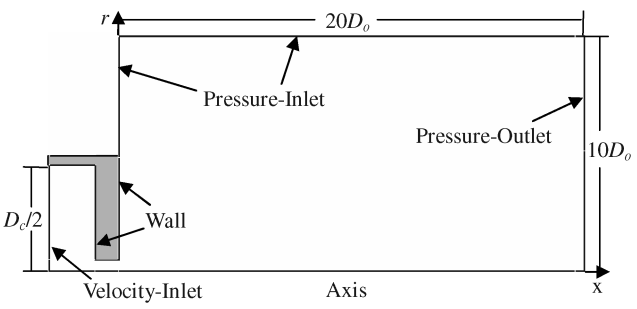

Fig. 2 Computational geometry and boundary conditions.

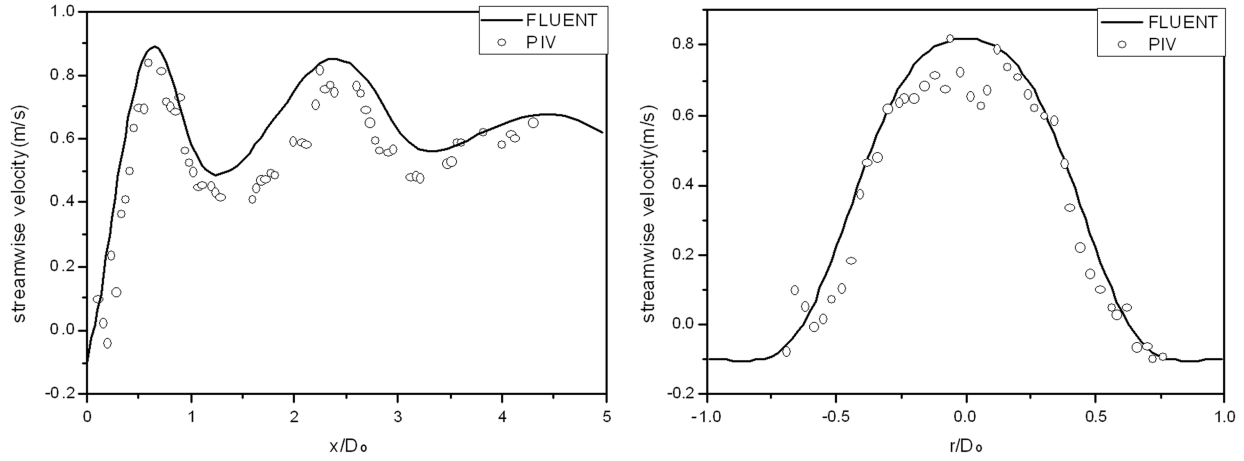

a) b)

Fig. 3 Comparisons of streamwise velocity a) along the jet centerline at $t/T = 9/16$ and b) in the spanwise direction at $x/D_o = 1$ and $t/T = 14/16$ with PIV data [15].

through the orifice during the blowing cycle [16]. The Stokes number is commonly defined as

$$S = \sqrt{\frac{2\pi f D_o^2}{\nu}} \tag{6}$$

It is found to determine the pressure losses due to friction as well as the entrance and exit flow in the orifice [17]. Because the Stokes number is related to L and Re_L via $Re_L = L^2S^2/2\pi$, only two of the preceding three dimensionless parameters are independent.

Along another line of thought, the importance of these three parameters can also be appreciated. The flow inside the actuator is dictated by the counteraction of three forces: inertia force, viscous force, and unsteady force. Here, the unsteady force is referred to as the force arising from the oscillating pressure field imposed by the oscillating diaphragm. If D_o, $\bar{U}_o$, and T are chosen as the characteristic length, velocity, and time scale, the representative inertia force, viscous force, and unsteady force in this case can be expressed as $\bar{U}_o^2/D_o$, $\nu\bar{U}_o/D_o^2$, and $\bar{U}_o/T$, respectively. The ratio of the inertia force and the unsteady force yields the dimensionless stroke length, justifying its appearance in the jet formation criterion as to if the inertia force overcomes the suction effect imposed by the unsteady force. Similarly, the ratio of the inertia force and viscous force gives the Reynolds number, justifying the use of the Reynolds number as an important parameter that determines the state of the jet as it comes out of the orifice [4]. Finally, the ratio of the unsteady force and viscous force gives the Stokes number. In the rest of this paper, it will be shown that the Stokes number is also an important parameter that affects the behavior of synthetic jets through the strength of vortex roll-up.

IV. Dimensionless Parameters Determining the Strength of Vortex Roll-Up

The formation of vortex rings is believed to be directly related to the evolution of the vortex sheet produced in the orifice [1]. When fluid is ejected from an orifice, a vortex sheet is formed that then proceeds to roll up into a vortex ring. The velocity across an idealized vortex sheet is discontinuous and consists of a continuous distribution of vortex lines. Crook [18] described the roll-up process as follows (see Fig. 4):

1) The vortex sheet induces a velocity on itself perpendicular to the plane of the sheet and this induced velocity is maximum at the leading edge of the sheet.

2) The self-induced velocity causes the leading edge of the sheet to curl.

3) The curled vortex sheet continues to induce a velocity component on the leading edge that, together with the normal component of the velocity induced by the uncurled sheet, is responsible for the roll-up observed in Fig. 4d.

Note that, in reality, the velocity jump across the vortex sheet is not discontinuous, due to the action of viscosity.

The strength of a vortex sheet can be measured by the level of vorticity Ω. Based on the definition of vorticity, if $\partial v/\partial x$ is ignored, the vorticity on a cylindrical vortex sheet can be expressed as

$$\Omega = \frac{\partial v}{\partial x} - \frac{\partial u}{\partial r} \approx -\frac{\partial u}{\partial r} \tag{7}$$

The order of magnitude of vorticity on the vortex sheet can be estimated as

$$\Omega \sim \frac{\bar{U}_o}{\varepsilon} = \frac{LfD_o}{\varepsilon} = Lf\frac{D_o}{\varepsilon} \tag{8}$$

where ε is the thickness of the Stokes layer in the orifice, which is defined as the radial distance between the position of the velocity peak and the wall at the orifice exit.

Taking into account the scale effect, one can get the dimensionless form of the vorticity:

$$\frac{\Omega D_o^2}{\nu} \sim L \cdot S^2 \cdot \frac{D_o}{\varepsilon} \tag{9}$$

Equation (9) reveals that the dimensionless vorticity is approximately proportional to the dimensionless stroke length L, Stokes number S, and ratio D_o/ε. It also indicates that to obtain a similar roll-up, vorticity Ω should be much higher for a synthetic jet issued from a smaller orifice. This is true because the vortex ring of small scale has a higher curvature, which demands a higher level of vorticity on the vortex sheet.

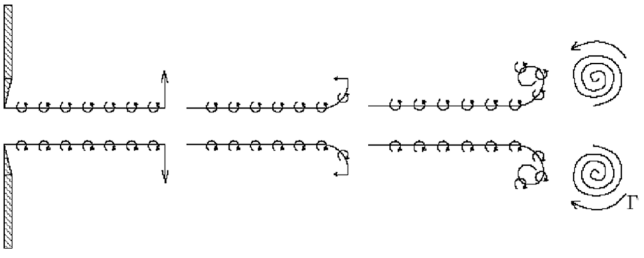

a) b) c) d)

Fig. 4 Idealized vortex ring formation: a) creation of vortex sheet through an orifice, b–c) curling up of the vortex sheet, and d) roll-up. Straight arrows represent induced velocity and small curved arrows represent vorticity [18].

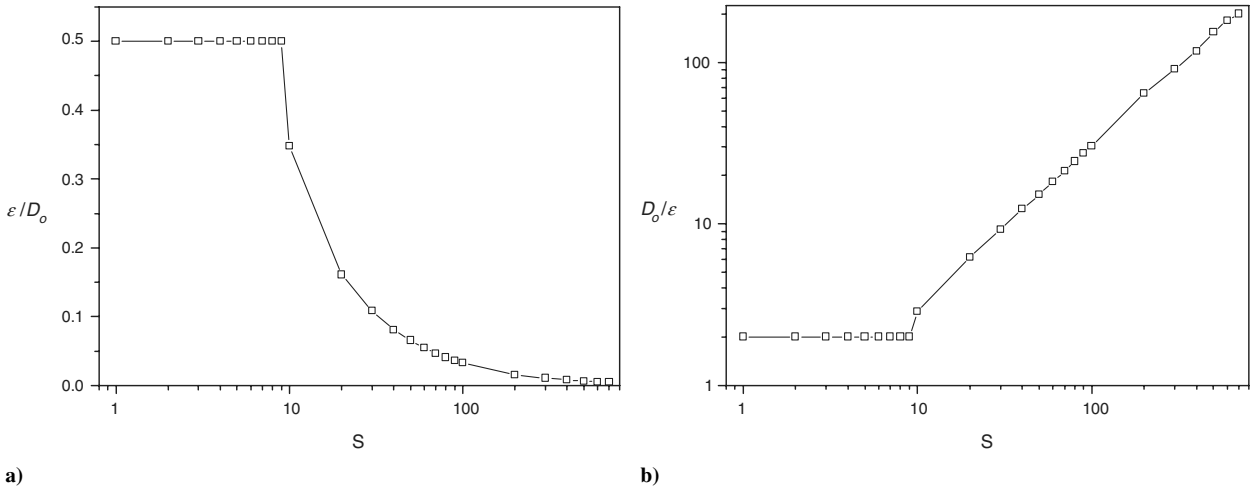

Fig. 5 Variation of the thickness of the Stokes layer in an oscillating pipe flow: a) ε/D_o vs S and b) D_o/ε vs S.

The integrated strength of the finite vortex sheet (i.e., the circulation of the vortex ring) can be estimated as

$$\Gamma \sim \Omega \cdot \varepsilon \cdot L_o \sim U_o L_o = (LfD_o) \cdot (LD_o) = L^2 f D_o^2 \tag{10}$$

Its nondimensional form becomes

$$\frac{\Gamma}{\nu} \sim L^2 \frac{fD_o^2}{\nu} = \frac{L^2 S^2}{2\pi} \sim Re_L \tag{11}$$

Equation (11) indicates that the dimensionless vortex circulation can be characterized by the Reynolds number Re_L, which is consistent with the previous finding by Glezer [4].

The normalized thickness of the Stokes layer ε/D_o is expected to depend on both L and S. Assuming a fully developed oscillating laminar pipe flow (i.e., the flow velocity does not change with the streamwise distance), ε/D_o is found to be a function of the Stokes number only. Figures 5a and 5b show the variation of ε/D_o and its inverse against the Stokes number S, respectively. Figure 5a indicates that the Stokes layer extends to the center of the orifice exit when $S < 10$, whereas it retreats rapidly toward the orifice wall as S increases above 10. As a measure of the ratio between the unsteady force and the viscous force, a higher Stokes number is expected to result in a thinner boundary layer along the orifice wall. Figure 5b shows that D_o/ε increases exponentially as S increases above 10. Hence, according to Eq. (9), the vorticity strength will subsequently experience a tremendous increase.

The thickness of the Stokes layer directly affects the location of the peak velocity in the velocity distribution and hence the exit velocity profile. This will affect the concentration of vorticity in the vortex sheet and hence its capability to form a vortex ring. At $S < 10$, the maximum velocity occurs at the center of the orifice exit and hence a thick cylindrical vortex sheet dominates the entire orifice. Consequently, the leading edge of the vortex sheet will be unable to curl, due to the axisymmetry and continuum of the flow. When S is greater than 10, however, a potential core appears at the center of the orifice, allowing the vortex sheet to curl and a vortex ring to form.

The preceding discussion is based on the assumption that the oscillating flow in the orifice is fully developed. For actuators in which the orifice depth-to-diameter ratio h/D_o is too small to allow the flow in the orifice to become fully developed, the requirement on the Stokes number loosens, because a potential core tends to exist due to the entrance effect.

V. Effects of the Dimensionless Parameters on Vortex Roll-Up of Synthetic Jets

Based on Eq. (9), both S and L will affect the strength of vortex roll-up. The aforementioned analysis reveals that for a fully developed oscillating orifice flow, the Stokes number plays an important role in determining the exit velocity profile and hence the tendency and strength of vortex roll-up. In this section, numerical simulations are used to illustrate the effect of changing S and L on the exit velocity profile and the strength of vortex roll-up of synthetic jets issued from an orifice with a finite length ($h/D_o = 1$) attached to a

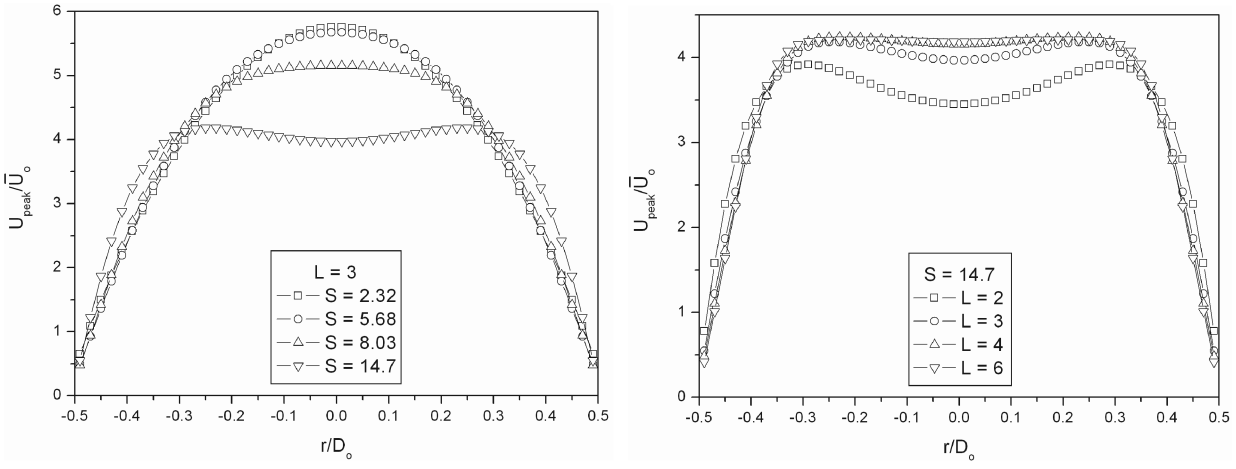

Fig. 6 Comparisons of exit velocity profiles of a synthetic jet at the phase of maximum expulsion at different a) Stokes numbers and b) dimensionless stroke lengths.

cavity. The simulations were undertaken on the actuator described in Sec. II for two groups of selected test cases in which either L or S was made the same by using different combinations of diaphragm displacements and frequencies. The exit velocity profiles normalized by the mean velocity $\bar{U}_o$ at the instant of maximum expulsion are then compared and the extent of vortex roll-up is examined.

As shown in Fig. 6a, at the same dimensionless stroke length ($L = 3$), the exit velocity profile changes gradually from a near-parabolic shape to a top-hat shape as S increases from 2.32 to 14.7. A similar trend was also observed in the experiment by Guo and Zhong [14]. The observed variation in the exit velocity profile is consistent with the finding from the fully developed oscillating flow discussed in the previous section; that is, an increasing Stokes number results in a decrease in the thickness of the Stokes layer. In Fig. 6b, the normalized velocity profiles at the same Stokes number ($S = 14.7$) but different L are compared. It is shown that the dimensionless stroke length also affects the shape of the exit velocity profiles considerably, especially the central part of the profile, although to a lesser extent. A lower L due to the use of a smaller diaphragm displacement results in a dip in the central region, which is commonly observed in an oscillating pipe flow. This phenomenon tends to enhance the effect of the Stokes number at low L, because the Stokes layer becomes thinner as a result of the velocity peak being closer to the wall (see Fig. 6b). As the dimensionless stroke length increases, the dip stretches itself out as a result of an increase in the jet momentum.

To illustrate how the extent of vortex roll-up is affected by the magnitude of the Stokes number, the flow fields at the corresponding

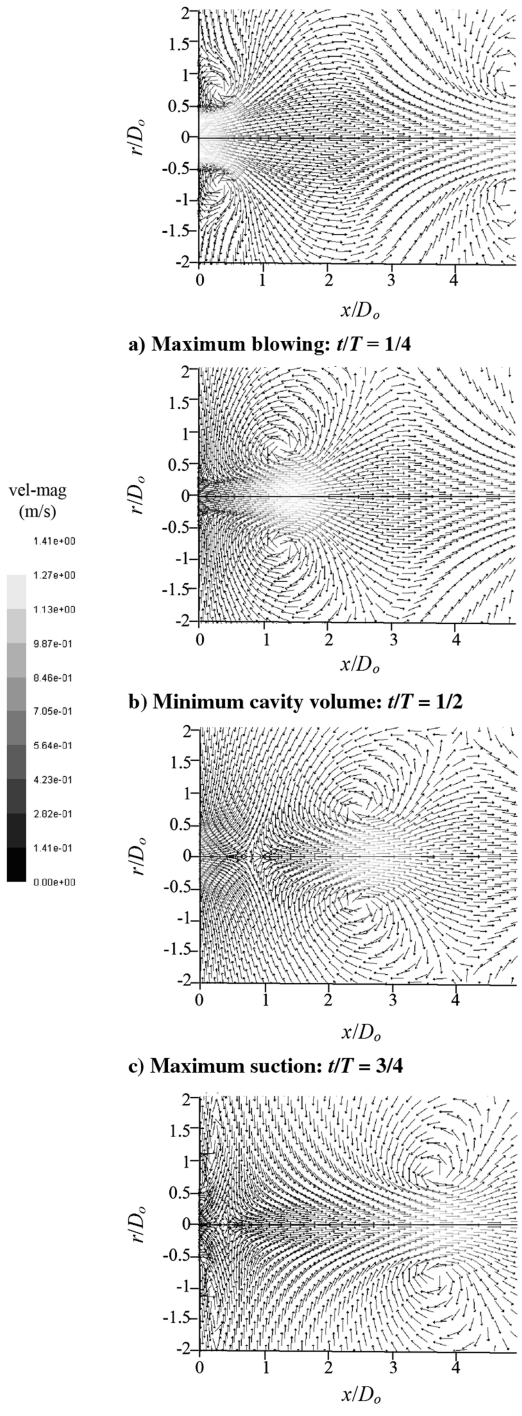

a) Maximum blowing: $t/T = 1/4$

b) Minimum cavity volume: $t/T = 1/2$

c) Maximum suction: $t/T = 3/4$

d) Maximum cavity volume: $t/T = 1$

Fig. 7 A time sequence of velocity vector field at $S = 14.7$ and $L = 3$.

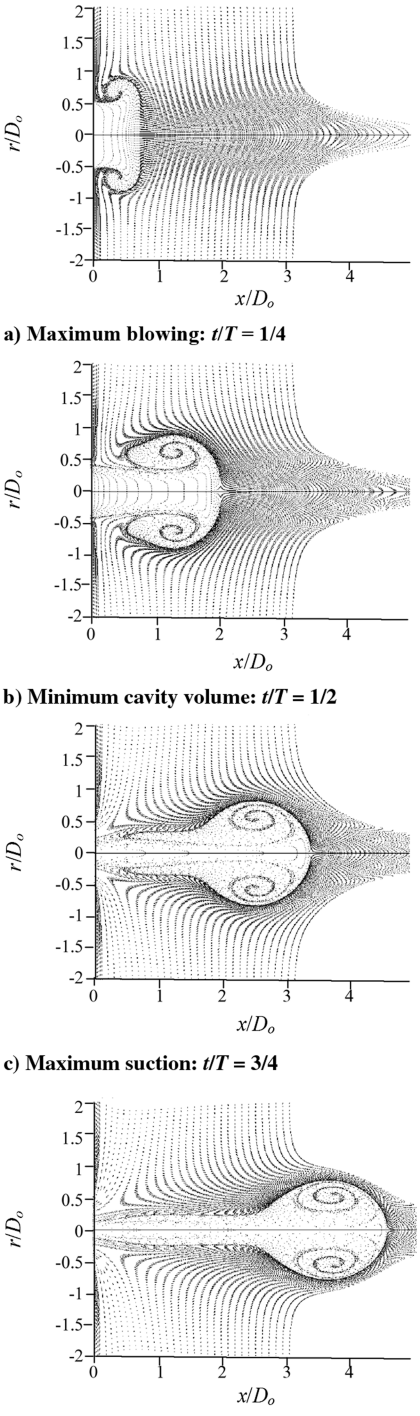

a) Maximum blowing: $t/T = 1/4$

b) Minimum cavity volume: $t/T = 1/2$

c) Maximum suction: $t/T = 3/4$

d) Maximum cavity volume: $t/T = 1$

Fig. 8 A sequence of patterns of timelines at $S = 14.7$ and $L = 3$.

test conditions in Fig. 6a are examined in detail. The velocity vector fields at four different phases during the diaphragm oscillation cycle at $S = 14.7$ are shown in Fig. 7. The velocity vectors are shaded with the local velocity magnitude. To make weak vortices more visible, velocity vectors of the same length are used, despite the differences in their velocity magnitudes. It can be seen at the maximum blowing phase (corresponding to the diaphragm at the neutral position in the blowing cycle) that a vortex pair associated with a strong rotational motion is formed at the orifice exit (see Fig. 7a). This vortex pair propagates downstream progressively, along with the central region of high velocity during the entire cycle.

To enable a confirmation of the presence of vortex roll-up, which is accompanied by entrainment of ambient fluid into the vortex core, the patterns of particle tracers at the corresponding phases are shown in Fig. 8. The particle tracers are released into the flow at short intervals of time from both the orifice exit and parallel lines in space, which are $0.02D_o$ apart outside the orifice. To allow the particles that originate from inside the orifice to be distinguished from those that originate from outside, the particles released from the orifice exit are shown in gray, and those from the outside are shown in black. At the phase of maximum blowing (Fig. 8a), the timelines on the wings of the structure, which is produced by the ejected fluid, curl upstream due to an intense local rotational motion. As the blowing cycle proceeds, the black tracers are seen to be drawn into the wings of this structure and swirl around it, indicating that the ambient flow near the orifice exit is being entrained into this structure. The location of the center of the vortex pair revealed by the velocity vectors appears to coincide with the region of the structure in which the ambient fluid is

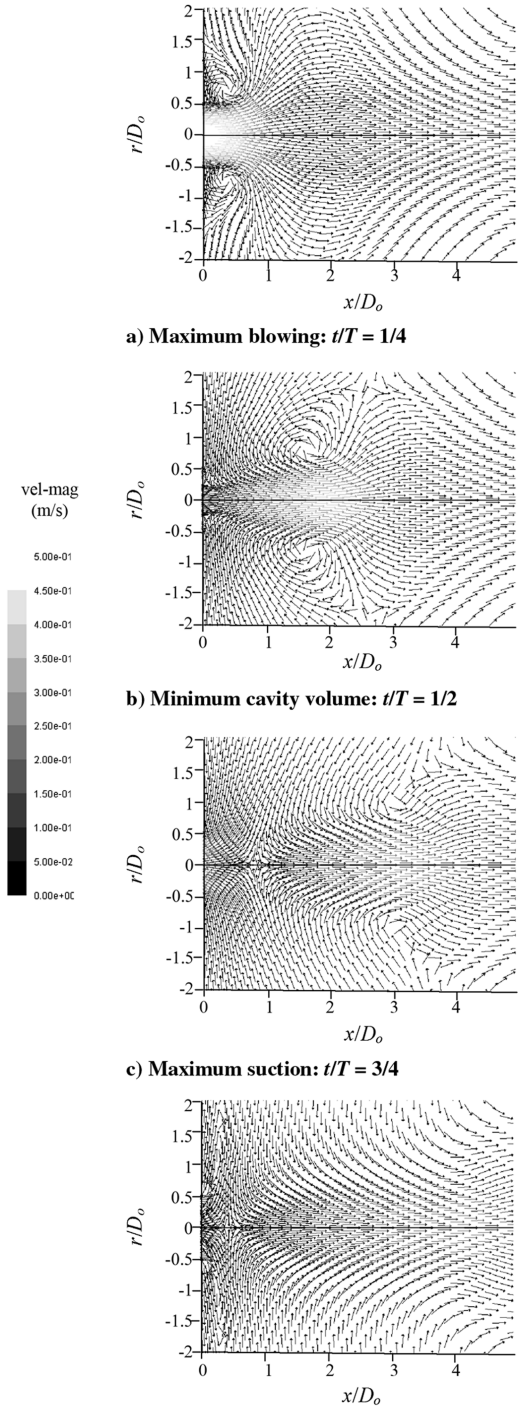

a) Maximum blowing: t/T = 1/4

b) Minimum cavity volume: t/T = 1/2

c) Maximum suction: t/T = 3/4

d) Maximum cavity volume: t/T = 1

Fig. 9 A time sequence of velocity vector field at $S = 8.03$ and $L = 3$.

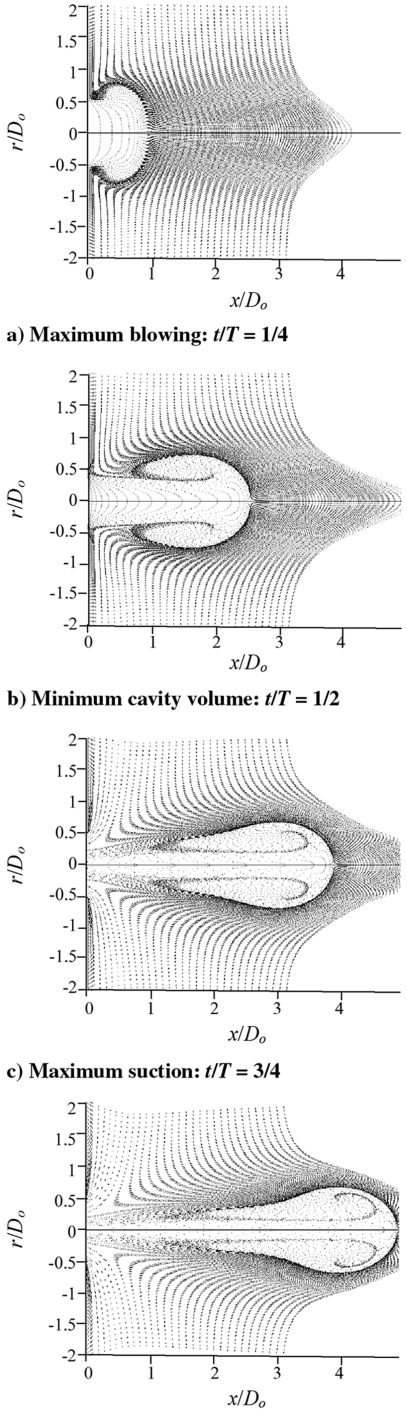

a) Maximum blowing: t/T = 1/4

b) Minimum cavity volume: t/T = 1/2

c) Maximum suction: t/T = 3/4

d) Maximum cavity volume: t/T = 1

Fig. 10 A sequence of patterns of timelines at $S = 8.03$ and $L = 3$.

entrained into, indicating that this vortex pair is responsible for the entrainment activity revealed by the timelines. This vortex pair is believed to be a part of a vortex ring caused by vortex roll-up of the ejected fluid from the orifice. This case is considered to be a typical case in which a strong vortex roll-up is present.

As the Stokes number is reduced to 8.03, a vortex pair similar to that observed at $S = 14.7$ also appears, although its strength is relatively weaker, as indicated by a smaller velocity magnitude (Fig. 9). The pattern of particle tracers (Fig. 10), however, indicates that the amount of entrainment brought about by this vortex pair is only marginal. Hence, this case is considered to be a transitional case for vortex roll-up.

At $S = 5.68$, a vortex pair also appears at the orifice exit at the phase of maximum blowing (Fig. 11a). It is weaker than those observed at $S = 8.03$ and 14.7, because it is associated with a lower velocity magnitude. The vortex pair disappears shortly downstream at the phase of maximum suction (corresponding to the diaphragm at the neutral position in the suction cycle) (see Fig. 11c). Although the timelines on the wings of the structure produced by the ejected fluid still curl toward the stem of the jet, a rotational motion is barely visible. In addition, almost no entrainment of ambient fluid is revealed by the particle tracers (Fig. 12). In fact, the vortex pair that is revealed by the velocity vectors appears to be located outside the region that is occupied by the fluid ejected from the orifice. Hence, it is not a part of a vortex ring. As the jet does appear to advance downstream during the cycle as shown by the timelines, this case is considered to be one that has jet formation but no vortex roll-up.

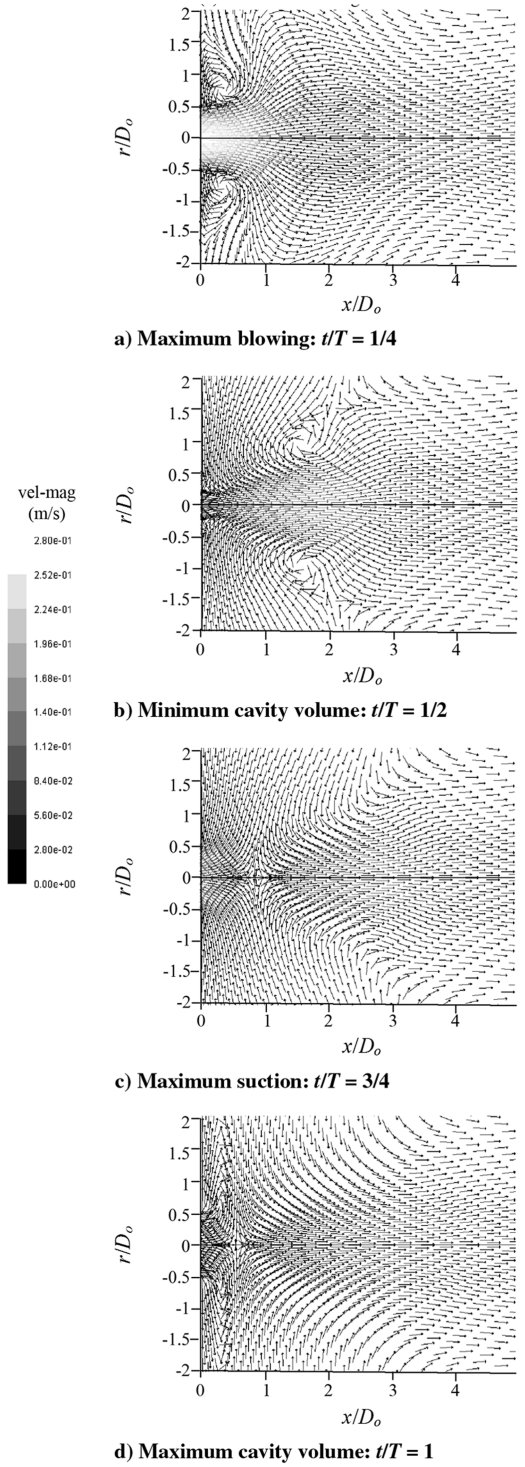

a) Maximum blowing: $t/T = 1/4$

b) Minimum cavity volume: $t/T = 1/2$

c) Maximum suction: $t/T = 3/4$

d) Maximum cavity volume: $t/T = 1$

Fig. 11 A time sequence of velocity vector field at $S = 5.68$ and $L = 3$.

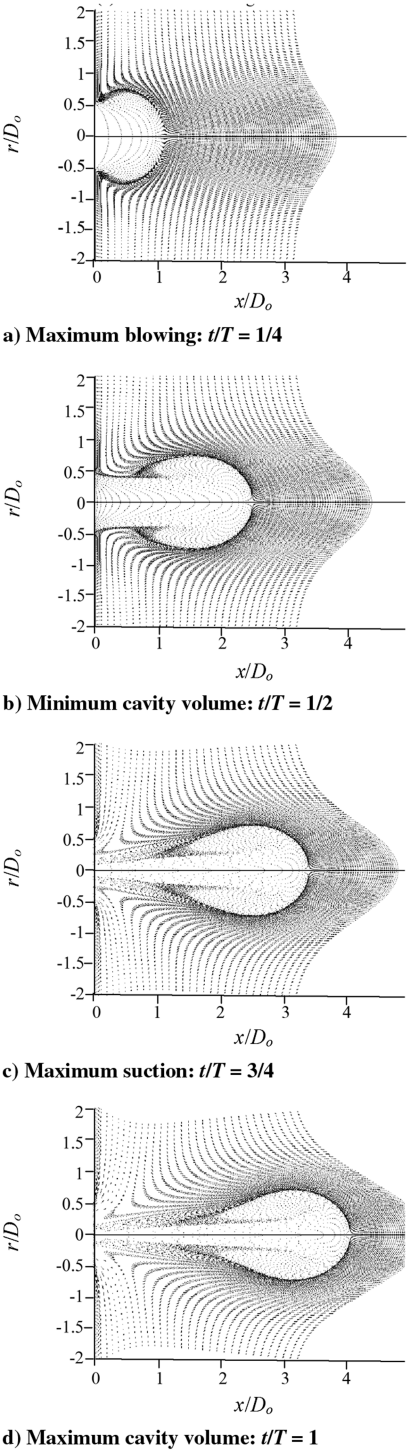

a) Maximum blowing: $t/T = 1/4$

b) Minimum cavity volume: $t/T = 1/2$

c) Maximum suction: $t/T = 3/4$

d) Maximum cavity volume: $t/T = 1$

Fig. 12 A sequence of patterns of timelines at $S = 5.68$ and $L = 3$.

It can be seen that a much weaker vortex pair of a similar nature to that observed at $S = 5.68$ also occurs at the smallest Stokes number, $S = 2.32$ (see Fig. 13a). The external timelines are deformed into an Ω shape in the blowing stroke, due to the fluid expulsed from the orifice exit (Figs. 14a and 14b). Again, no entrainment of ambient fluid into the flow structure produced by the jet is seen. During the suction cycle, a substantial amount of ejected fluid is ingested into the cavity such that the most downstream part of the timelines shows no forward movement during the entire cycle, indicating that the jet does not propagate away from the orifice (Figs. 14c and 14d). Hence, a synthetic jet is not formed.

Figure 15 shows the instantaneous centerline streamwise velocity for the corresponding cases in Figs. 7–14 at four phases. At $S = 2.32$, the magnitude of the streamwise velocity at the centerline decreases sharply at all phases and drops to almost zero within a distance of approximately $2D_o$ from the orifice (see Fig. 15a), confirming that no jet is formed in this case. At $S = 5.68$, the magnitude of velocity fluctuations is a lot higher (Fig. 15b). Although its value indicates the presence of only one distinct structure and a subsequent rapid decay within $4D_o$ from the orifice, a nonzero streamwise velocity is observed at a distance of $12D_o$ downstream from the orifice exit. Hence, a synthetic jet should have been formed despite its weak strength. As S increases further, the magnitude of velocity not only increases, but multiple velocity peaks are also observed, indicating the propagation of a train of structures downstream (see Figs. 7b and 7c). This is what would be expected when vortex rings are formed.

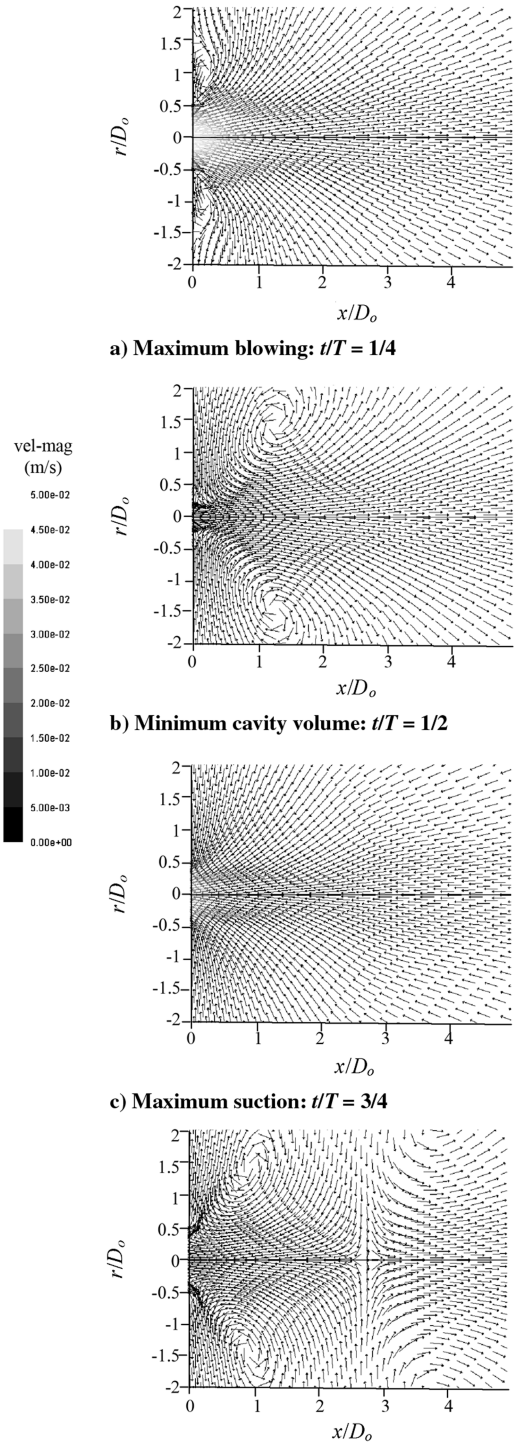

a) Maximum blowing: t/T = 1/4

b) Minimum cavity volume: t/T = 1/2

c) Maximum suction: t/T = 3/4

d) Maximum cavity volume: t/T = 1

Fig. 13 A time sequence of velocity vector field at $S = 2.32$ and $L = 3$.

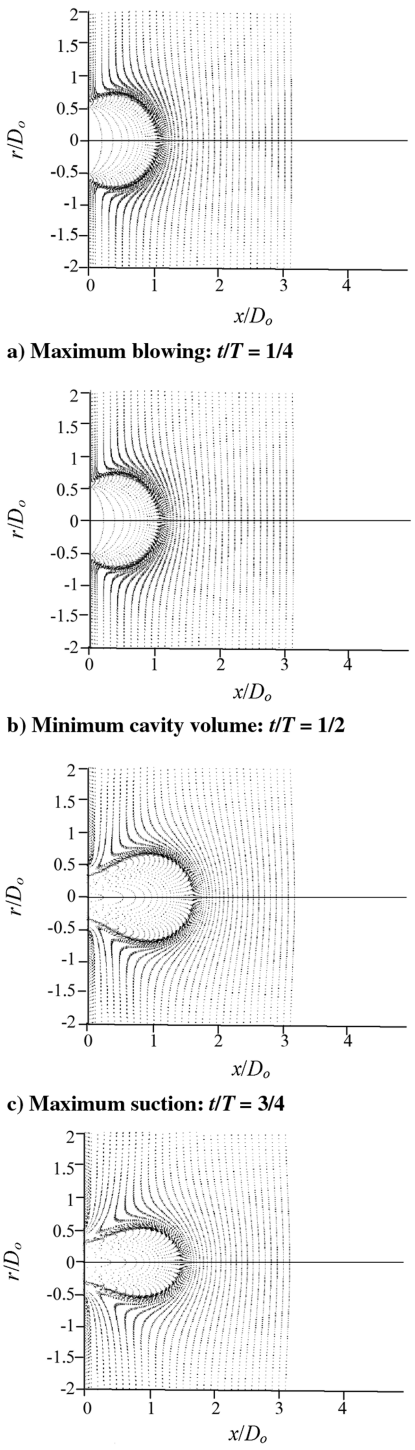

a) Maximum blowing: t/T = 1/4

b) Minimum cavity volume: t/T = 1/2

c) Maximum suction: t/T = 3/4

d) Maximum cavity volume: t/T = 1

Fig. 14 A sequence of patterns of timelines at $S = 2.32$ and $L = 3$.

From the preceding discussion of the four cases, it can been seen that when the dimensionless stroke length is kept constant, as the Stokes number increases, the synthetic jets go through three different regimes from no jet formation, to jet formation without vortex roll-up, to jet formation with vortex roll-up. The near-parabolic exit velocity profile at $S = 2.32$ and 5.68 is believed to be the reason that no vortex roll-up is observed in these cases, because a thick Stokes layer inhibits the curling up of vortex sheets required for the formation of a vortex ring. Based on the preceding visual impressions, it is confirmed that a minimum Stokes number is required for an appreciable roll-up to occur within the range of dimensionless stroke length examined here. Furthermore, note that although the dimensionless stroke length L is 3, which is well above the jet formation criterion of $L = 0.5$ proposed by Holman et al. [10], a jet formation fails to occur at $S = 2.32$ (see Figs. 13 and 14). Hence, it appears that the Stokes number also has to be large enough to ensure jet formation even at a large stroke length.

As shown in Eq. (11), the Reynolds number Re_L characterizes the level of vortex circulation of a synthetic jet. The current study suggests, however, that there is an exception when the Stokes number is below a threshold value. Figure 16 shows the vorticity contour superimposed on the velocity vector field for two test cases, which have the same Reynolds number ($Re_L = 137$) but different S and hence two distinctly different exit velocity profiles. At $S = 14.7$, the exit velocity profile has a top-hat shape, and the core of the roll-up vortex is found to almost coincide with the location of peak vorticity. Because the potential core is irrotational, all circulation produced by the blowing part of the cycle is likely to be contained in the vortex ring. At $S = 7.35$, however, the exit velocity profile has a near-parabolic shape. At this Stokes number, an offset exists between the center of the vortex roll-up and the location of peak vorticity in the shear layer. It appears that only a small portion of the total circulation produced by the blowing part of the cycle is accumulated in the vortex and the rest is deposited in the shear layer that extends to the jet centerline. This suggests that although Re_L determines the total circulation ejected through the orifice, the Stokes number moderates the proportion that will be collected in the initial roll-up. Nevertheless, when the Stokes number is sufficiently high such that a predominant potential core is present in the jet flow, it may become more adequate to state that the Reynolds number determines the roll-up strength, because a majority of the total circulation is pumped into the vortex ring.

VI. Parameter Map for Jet Formation and Vortex Roll-Up

From the preceding discussion, it has become clear that the Stokes number plays an important role in determining the strength of vortex roll-up of a synthetic jet, because it significantly affects the shape of the exit velocity profile. It appears that the Stokes number also has to be large enough to ensure jet formation even at a large dimensionless stroke length. To appreciate the effect of both Stokes number and dimensionless stroke length on the state of a synthetic jet, it is useful to establish a parameter space in which the different regimes of synthetic jets classified as no jet formation, jet formation without roll-up, and jet formation with vortex roll-up are identified for the present actuator.

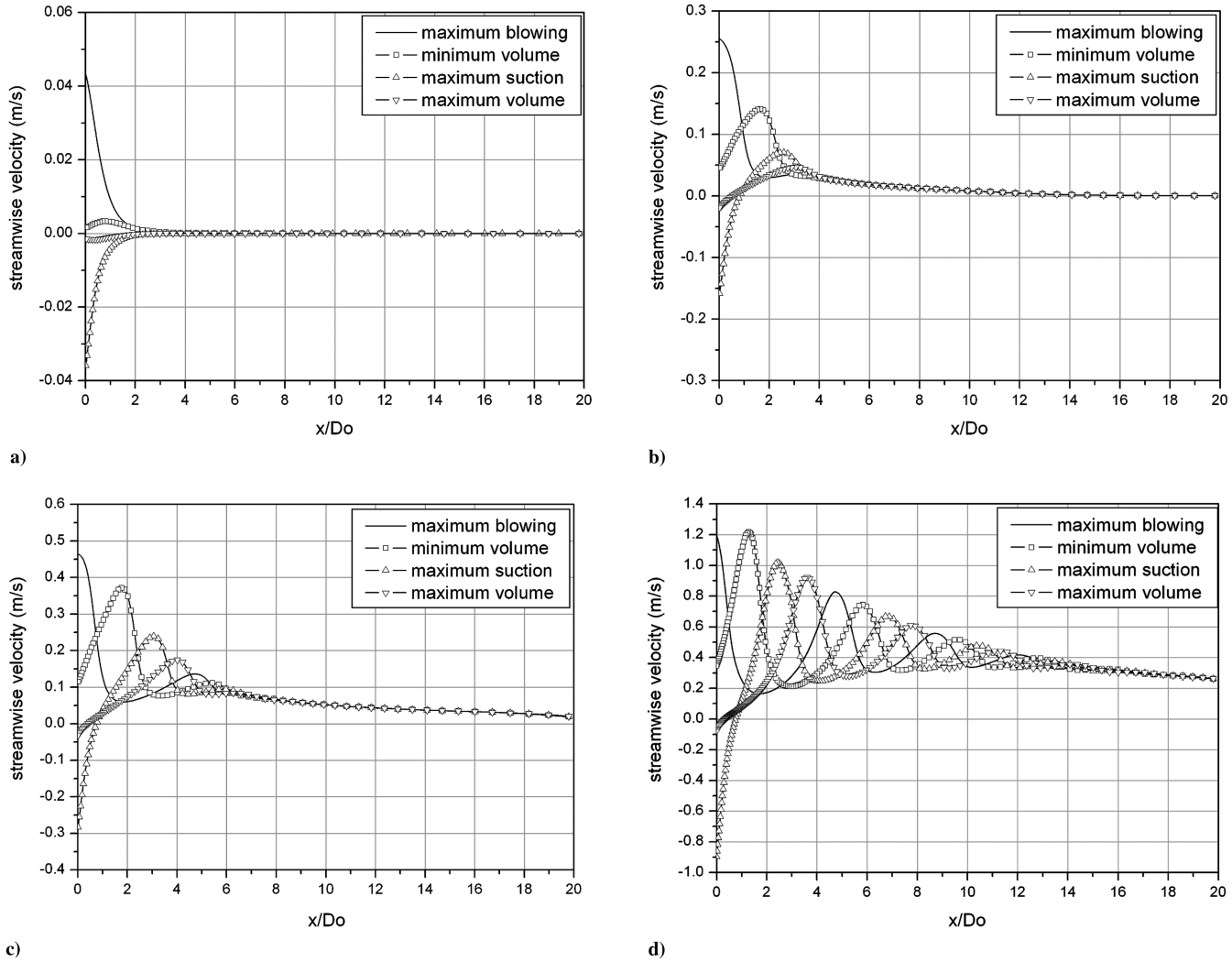

Fig. 15 Instantaneous streamwise velocities at the jet centerline for the cases at $L = 3$: a) $S = 2.32$, b) $S = 5.68$, c) $S = 8.03$, and d) $S = 14.7$.

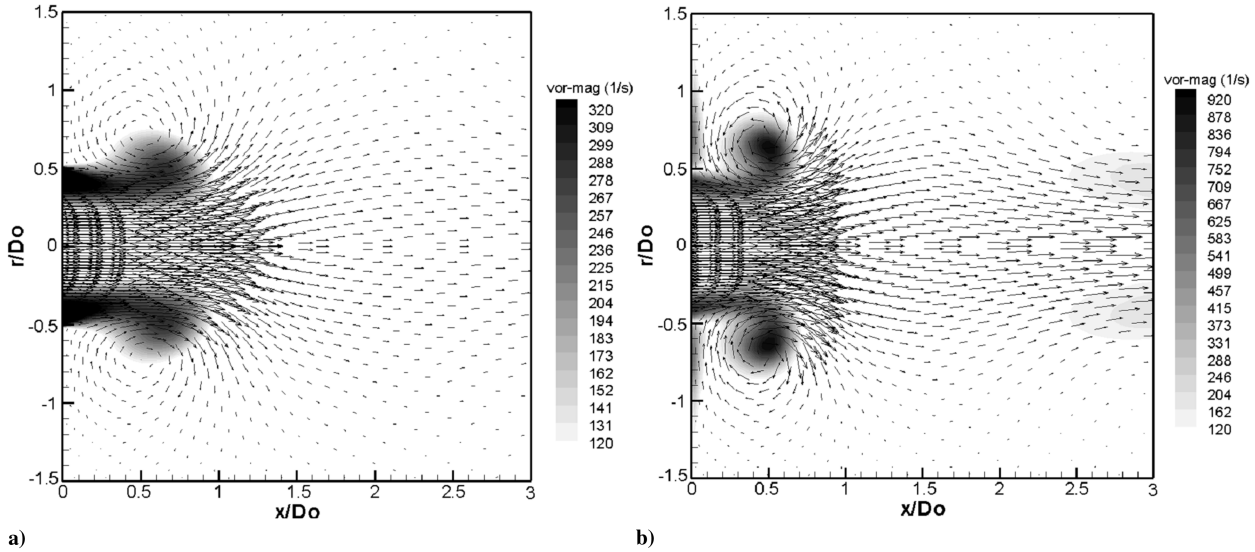

Fig. 16 Comparison of synthetic jets at the same Re_L showing how the Stokes number moderates the strength of vortex roll-up: a) $L = 4$ and $S = 7.35$ ($Re_L = 137$) at $t/T = 1/4$ and b) $L = 2$ and $S = 14.7$ ($Re_L = 137$) at $t/T = 3/8$.

In this study, numerical simulations of 70 cases have been undertaken using different combinations of diaphragm displacements and frequencies that cover the range of $0.5 < L < 10$ and $2 < S < 26$. The timeline method described in the previous section is used to display the results and to determine the state of the synthetic jets in a semi-qualitative manner. A parameter map containing all the test cases is shown in Fig. 17. The parameter map can be divided into three regimes, corresponding to no jet formation, jet formation without vortex roll-up, and jet formation with vortex roll-up. Transitional boundaries between different regimes are obtained by best fitting the data shown in Fig. 17.

From this graph it is seen that the synthetic jet cannot be formed when the Stokes number is low, even at very high stroke lengths, and the threshold value of Stokes number for jet formation increases as the dimensionless stroke length decreases. A best fit of the boundary between no jet and jet formation without roll-up shows that on the boundary, $S \propto L^{-0.62}$. It is believed that the reason that the jet does not form at very low Stokes numbers is the viscous effect being too high to allow the periodic formation of the jet. In the jet formation criterion proposed by Holman et al. [10], only the counteraction of the inertia force and the unsteady force is considered, resulting in the dimensionless stroke length being the only parameter that affects jet formation.

For the present actuator, jet formation is observed at the dimensionless stroke length of $L = 1$ when $S > 7.5$. Here, a boundary between no jet formation and jet formation without vortex roll-up is drawn at $L = 0.5$ on the graph based on the formation criterion given by Holman et al. [10].

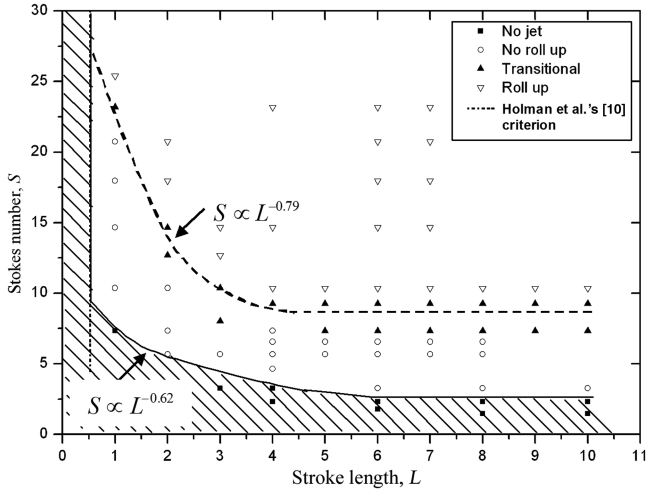

Fig. 17 Parametric map showing different regimes of synthetic jet formation.

There is a reasonably well-defined transitional boundary separating the jets with and without vortex roll-up. For $L < 4$, the threshold of S for vortex roll-up increases as the dimensionless stroke length decreases. The transitional boundary has an expression of $S \propto L^{-0.79}$. For $L > 4$, the transitional boundary is asymptotic to a horizontal line at about $S = 8.5$, suggesting that the threshold of S for vortex roll-up remains constant at large L. Hence, at large dimensionless stroke lengths, the Stokes number is the only parameter that determines if a vortex roll-up will occur. The need to have a sufficiently high Stokes number for vortex roll-up to occur in a synthetic jet is consistent with the finding from the theoretical analysis of a fully developed oscillating pipe flow discussed in Sec. IV. The slightly lower threshold value than the theoretical predicted value of 10 is believed to be caused by the relatively short length of the orifice, which encourages the exit velocity profile to acquire a top-hat shape. Note that the threshold value of $S = 8.5$ for vortex roll-up is obtained specifically for the synthetic jet actuator studied in this paper. Hence, a deviation from this value is expected for actuators that have a different orifice lip shape, orifice depth-to-diameter ratio, and velocity program.

According to its definition, the Stokes number decreases linearly with the orifice diameter and increases linearly with the square root of the actuation frequency. Because the orifice diameter is expected to be in the range of a few tenths or hundredths of a millimeter for flow control purposes in aerospace applications, the Stokes number may become undesirably low with the use of a very small orifice, resulting in no vortex roll-up or even no jet formation. Based on the finding from this study, to ensure the flow control effectiveness of synthetic jets in practical settings, as the scale of the actuator reduces, the actuator operating frequency has to increase substantially to satisfy the condition for vortex roll-up. On the other hand, because the displacement of an actuator driven by a piezoelectric diaphragm decreases significantly at high frequencies, achieving a sufficient dimensionless stroke length to ensure jet formation can also become more challenging. Therefore, both the jet formation criterion and the vortex roll-up criterion should be considered in conjunction with each other when one is designing the synthetic jet actuators for aerospace applications.

VII. Conclusions

In this paper, both theoretical analysis and numerical simulations are undertaken to study the parameters that affect the strength of

vortex roll-up of synthetic jets. First, a dimensional analysis reveals that the dimensionless vorticity of vortex roll-up produced by an orifice flow depends on the dimensionless stroke length, Stokes number, and the ratio between the orifice diameter and the thickness of the Stokes layer. Based on the results from a fully developed oscillating laminar pipe flow, the Stokes number is found to play an important role in determining the thickness of the Stokes layer inside the orifice and hence the shape of the velocity profile. Results from the numerical simulations confirm that the Stokes number also determines the strength of vortex roll-up of a synthetic jet issued from an orifice of a finite depth, for the same reason. Finally, a parameter map, which marks the three different regimes of synthetic jets classified as no jet, jet formation without vortex roll-up, and jet formation with vortex roll-up, is produced based on the numerical simulation results. It is shown that for the synthetic jet actuator used in the present study, a minimum Stokes number of about 8.5 is required to ensure the occurrence of an appreciable vortex roll-up at a dimensionless stroke length greater than 4. In addition, a very low Stokes number can also suppress the formation of synthetic jets. This study provides a more in-depth understanding of the behavior of synthetic jets in quiescent conditions, which will be useful for designing more effective synthetic jet actuators in which vortex roll-up is desired.

References

[1] Shariff, K., and Leonard, A., "Vortex Rings," *Annual Review of Fluid Mechanics*, Vol. 24, 1992, pp. 235–279. doi:10.1146/annurev.fl.24.010192.001315

[2] Pullin, D. I., "Vortex Ring Formation at Tube and Orifice Openings," *Physics of Fluids*, Vol. 22, No. 3, Mar. 1979, pp. 401–403. doi:10.1063/1.862606

[3] Didden, N., "On the Formation of Vortex Rings: Rolling-up and Production of Circulation," *Zeitschrift fur Angewandte Mathematik und Physik (1982)*, Vol. 30, 1979, pp. 101–116. doi:10.1007/BF01597484

[4] Glezer, A., "The Formation of Vortex Rings," *Physics of Fluids*, Vol. 31, No. 12, Dec, 1988, pp. 3532–3542. doi:10.1063/1.866920

[5] Gharbi, M., Rambod, E., and Shariff, K., "A Universal Time Scale for Vortex Ring Formation," *Journal of Fluid Mechanics*, Vol. 360, 1998, pp. 121–140. doi:10.1017/S0022112097008410

[6] Smith, B. L., and Glezer, A., "The Formation and Evolution of Synthetic Jets," *Physics of Fluids*, Vol. 10, No. 9, Sept. 1998, pp. 2281–2297. doi:10.1063/1.869828

[7] Glezer, A., and Amitay, M., "Synthetic Jets," *Annual Review of Fluid Mechanics*, Vol. 34, 2002, pp. 503–529. doi:10.1146/annurev.fluid.34.090501.094913

[8] Zhong, S., Jabbal, M., Tang, H., Garcillan, L., Guo, F., Wood, N. J., and Warsop, C., "Towards the Design of Synthetic-Jet Actuators for Full-Scale Flight Conditions. Part 1: The Fluid Mechanics of Synthetic-Jet Actuators," *Flow, Turbulence and Combustion*, Vol. 78, No. 3, 2007, pp. 283–307. doi:10.1007/s10494-006-9064-0

[9] Tang, H., Zhong, S., Jabbal, M., Garcillan, L., Guo, F., Wood, N. J., and Warsop, C., "Towards the Design of Synthetic-Jet Actuators for Full-Scale Flight Conditions. Part 2: Low-Dimensional Actuator Prediction Models and Actuator Design Methods," *Flow, Turbulence and Combustion*, Vol. 78, No. 3, 2007, pp. 309–329. doi:10.1007/s10494-006-9061-3

[10] Holman, R., Utturkar, Y., Mittal, R., Smith, B. L., and Cattafesta, L., "Formation Criterion for Synthetic Jets," *AIAA Journal*, Vol. 43, No. 10, 2005, pp. 2110–2116. doi:10.2514/1.12033

[11] Milanovic, I. M., and Zaman, K. B. M. Q., "Synthetic Jets in Crossflow," *AIAA Journal*, Vol. 43, No. 5, 2005, pp. 929–940. doi:10.2514/1.4714

[12] Zhou, J., and Zhong, S., "Numerical Simulation of the Interaction of a Circular Synthetic Jet with a Boundary Layer," *Computers and Fluids*, Vol. 38, No. 2, 2009, pp. 303–405. doi:10.1016/j.compfluid.2008.04.012

[13] Jabbal, M., and Zhong, S., "The Near Wall Effect of Synthetic Jets in a Boundary Layer," *International Journal of Heat and Fluid Flow*, Vol. 29, No. 1, 2008, pp. 119–130. doi:10.1016/j.ijheatfluidflow.2007.07.011

[14] Guo, F., and Zhong, S., "A PIV Investigation of the Characteristics of Micro-Scale and Macro-Scale Synthetic Jets," AIAA Paper 2006-3183, June 2006.

[15] Tang, H., and Zhong, S., "2D Numerical Study of Circular Synthetic Jets in Quiescent Conditions," *The Aeronautical Journal*, Vol. 109, No. 1092, 2005, pp. 89–97.

[16] Tang, H., and Zhong, S., "Incompressible Flow Model of Synthetic Jet Actuators," *AIAA Journal*, Vol. 44, No. 4, 2006, pp. 908–912. doi:10.2514/1.15633

[17] Raju, R., Gallas, Q., Mittal, R., and Cattafesta, L., "Scaling of Pressure Drop for Oscillatory Flow Through a Slot," *Physics of Fluids*, Vol. 19, 2007, Paper 078107. doi:10.1063/1.2749814

[18] Crook, A., "The Control of Turbulent Flows Using Synthetic Jets," Ph.D. Dissertation, School of Engineering, Univ. of Manchester, Manchester, England, U.K., 2002.

A. Plotkin
Associate Editor